Обзор ArXiv: astro-ph, 16-20 февраля 2018 года

От Сильченко О.К.

Astro-ph: 1802.04043

The HIX galaxy survey II: HI kinematics of HI eXtreme galaxies

K. A. Lutz,[1,2⋆] V. A. Kilborn,[1] B. S. Koribalski,[2] B. Catinella,[3]
G. I. G. Józsa,[4,5,6] O. I. Wong, [3] A. R. H. Stevens,[1,3] D. Obreschkow,[3]
H. Dénes, [2,7]

[1] *Centre for Astrophysics and Supercomputing, Swinburne University of Technology, P.O. Box 218, Hawthorn, VIC 3122, Australia*
[2] *Australia Telescope National Facility, CSIRO Astronomy and Space Science, P.O. Box 76, Epping, NSW 1710, Australia*
[3] *International Centre for Radio Astronomy Research (ICRAR), M468, The University of Western Australia, 35 Stirling Highway, Crawley, WA 6009, Australia*
[4] *SKA South Africa Radio Astronomy Research Group, 3rd Floor, The Park, Park Road, Pinelands 7405, South Africa*
[5] *Rhodes Centre for Radio Astronomy Techniques & Technologies, Department of Physics and Electronics, Rhodes University, PO Box 94, Grahamstown 6140, South Africa*
[6] *Argelander-Institut für Astronomie, Auf dem Hügel 71, D-53121 Bonn, Germany*
[7] *Research School of Astronomy and Astrophysics, The Australian National University, Canberra, ACT 2611, Australia*

Accepted XXX. Received YYY; in original form ZZZ

ABSTRACT

By analysing a sample of galaxies selected from the HI Parkes All Sky Survey (HIPASS) to contain more than 2.5 times their expected HI content based on their optical properties, we investigate what drives these HI eXtreme (HIX) galaxies to be so HI-rich. We model the HI kinematics with the *Ti*lted *Ring Fi*tting *C*ode TiRiFiC and com-

Выборка

HI-rich

2.1 Galaxy samples

In this paper, we perform a kinematic analysis of galaxies in the HIX survey, which was first presented in Lutz et al. (2017). HIX galaxies were selected as a subsample of the compilation presented by Dénes et al. (2014), who used their sample to calibrate scaling relations between H I mass and optical luminosity. This parent sample consists of 1796 galaxies from the HIPASS catalogues (Meyer et al. 2004; Koribalski et al. 2004), which have reliable optical counterparts in HOPCAT (Doyle et al. 2005).

In our 2017 paper, HIX and control samples included 13 galaxies each. HIX galaxies were selected to lie at least $1.4\,\sigma$ above the Dénes et al. (2014) scaling relation between H I mass and absolute R-band magnitude. The control sample has been selected from the same parent sample to lie within $\pm 0.7\,\sigma$ of the scaling relation. We exclude dwarf galaxies by restricting our sample to stellar masses greater than $\log M_\star\,[M_\odot] > 9.7$. In this paper, control galaxies NGC 4672, IC 4366 and ESO462-G016 are excluded because the signal to noise ratio of their H I data was too low.

ID	θ_1 [″]	θ_2 [″]	rms [mJy beam^{-1}]
(1)	(2)	(3)	(4)
ESO111-G014	52.66	40.58	1.7
ESO243-G002	31.70	22.95	1.5
NGC 289[a]	55.98	25.64	1.4
ESO245-G010	51.48	31.30	1.7
ESO417-G018	66.09	33.33	1.6
ESO055-G013	43.08	33.54	2.0
ESO208-G026	59.24	43.49	1.3
ESO378-G003	64.23	41.09	1.3
ESO381-G005	65.76	43.50	1.5
ESO461-G010[b]	59.62	29.38	2.7
ESO075-G006	60.52	35.22	2.0
ESO290-G035[b]	58.32	28.98	2.1
NGC 685	34.58	32.48	1.9
ESO121-G026[c]	25.42	18.91	0.6
ESO123-G023	35.74	28.94	2.3
NGC 3001[c]	38.49	20.97	1.3
ESO263-G015	25.53	22.60	3.0
NGC 3261	56.50	39.31	2.7
NGC 5161[c]	36.59	20.41	1.3
ESO383-G005	40.83	22.02	2.8
IC 4857	40.16	26.92	1.1
ESO287-G013	38.00	30.33	2.0
ESO240-G011	29.32	22.87	3.0

контрольная

NGC 289: HI-rich

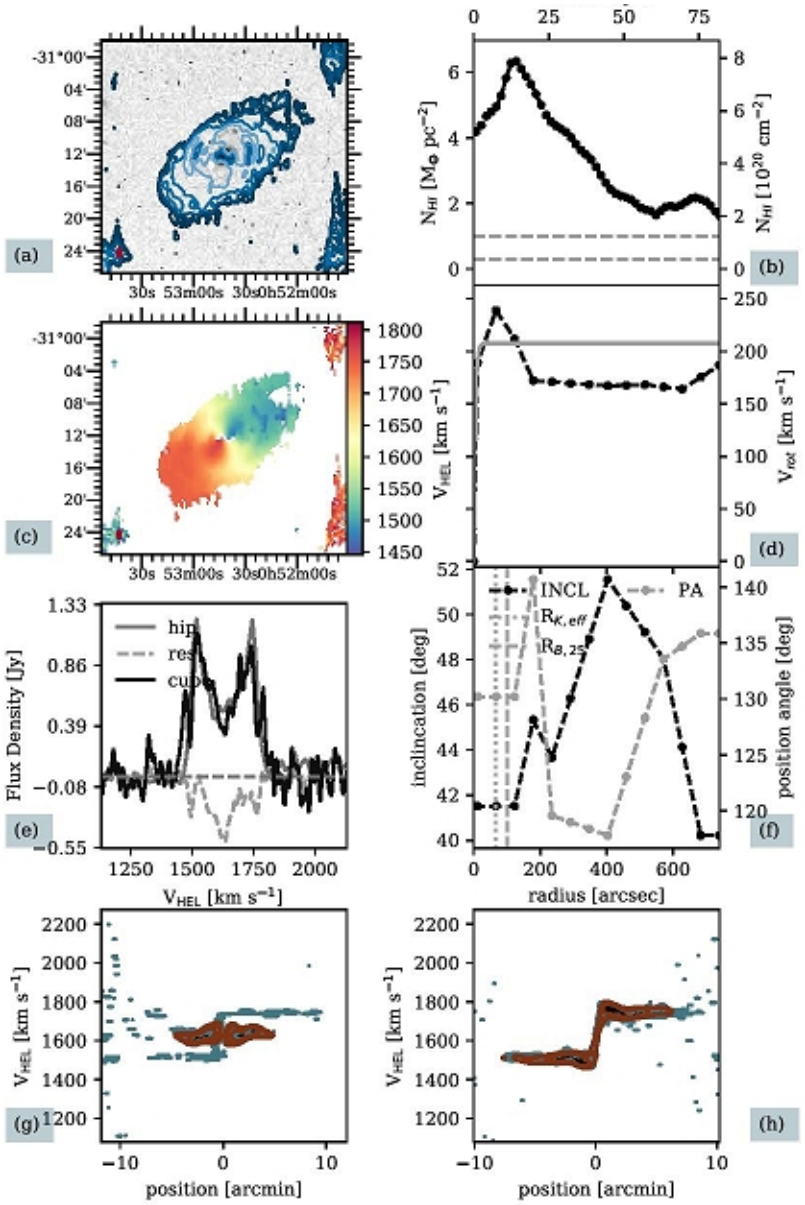

Figure A3. NGC289

- Плотность HI
- Скорости HI
- Результаты TiRiFic
- P-V диаграммы вдоль малой (слева) и большой (справа) оси

Примеры из контрольной выборки

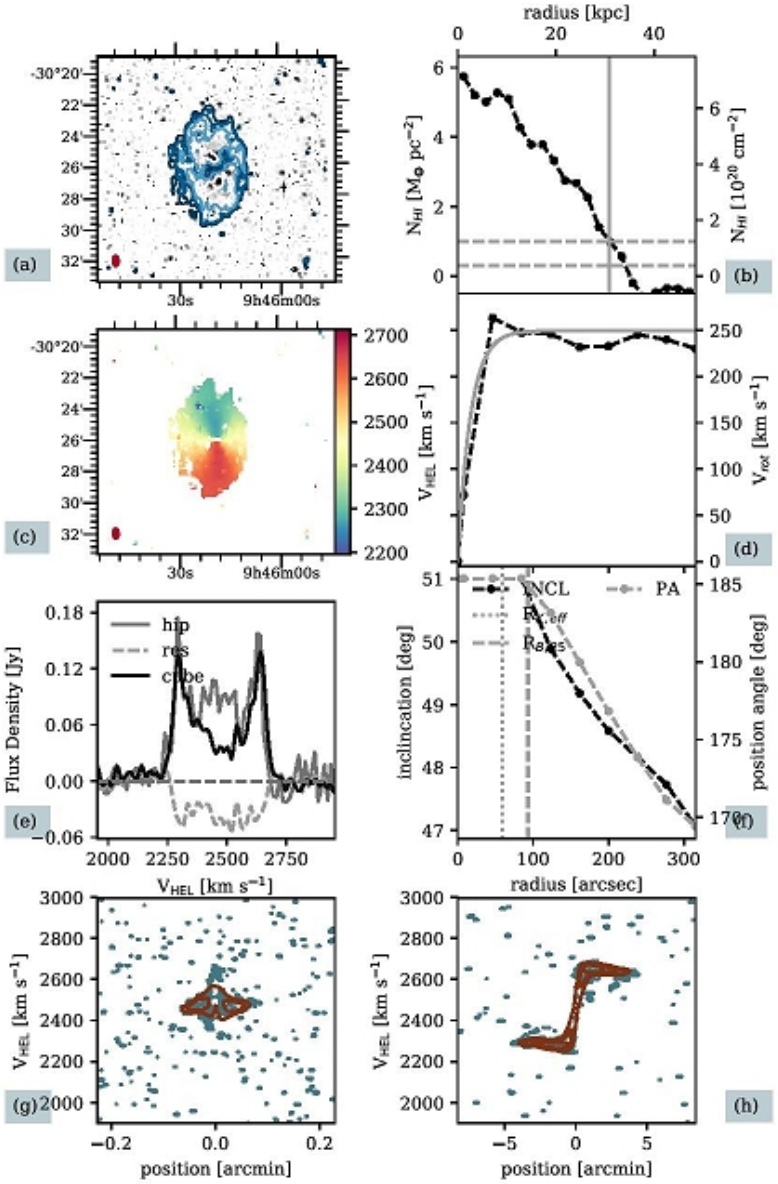

Figure B4. NGC3001

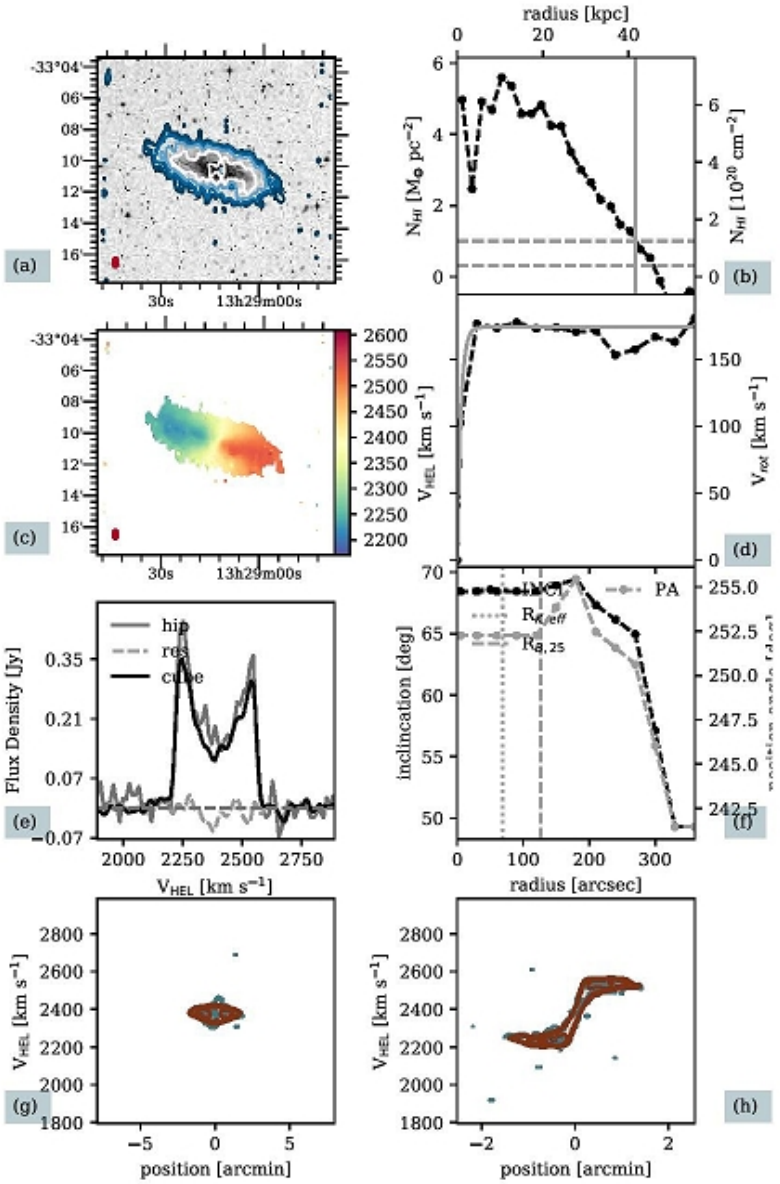

Figure B7. NGC5161

Свойства выборки

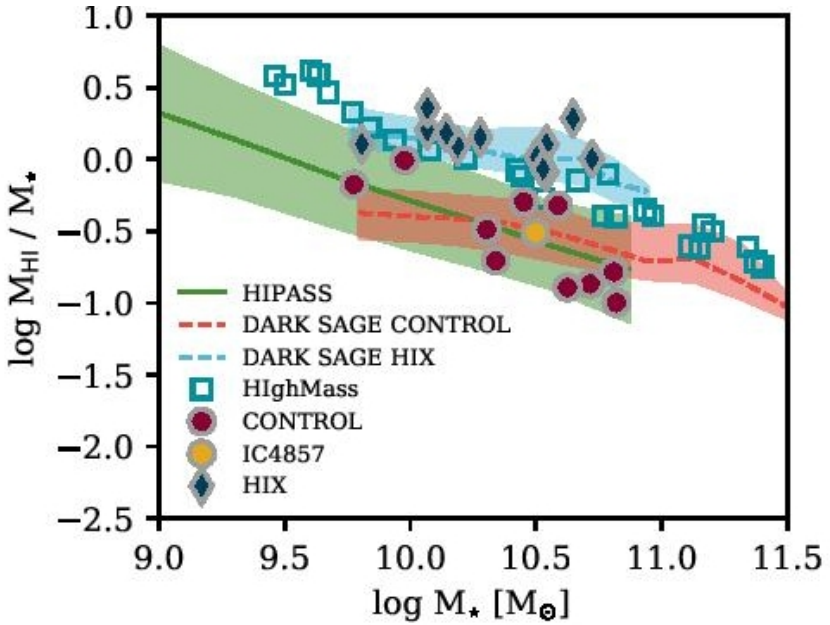

Figure 1. The H I–to–stellar mass ratio as a function of the stellar mass. The green shaded area shows the 1 σ range of the parent sample (with 2MASS cross match), red circles give the control sample and blue diamonds represent the HIX sample. The yellow circle is IC 4857, which was initially selected as a HIX galaxy, but then reclassified to a control galaxy. The empty blue squares present the HIghMass sample. Orange and light blue dashed lines indicate the running average of simulated HIX (light blue) and control galaxies (orange) from the DARK SAGE semi-analytic model (for more details see Sec. 4). The orange and light blue shading covers the 16 to 84 percentile range. As per sample selection, HIX galaxies have high H I mass fractions for their stellar mass.

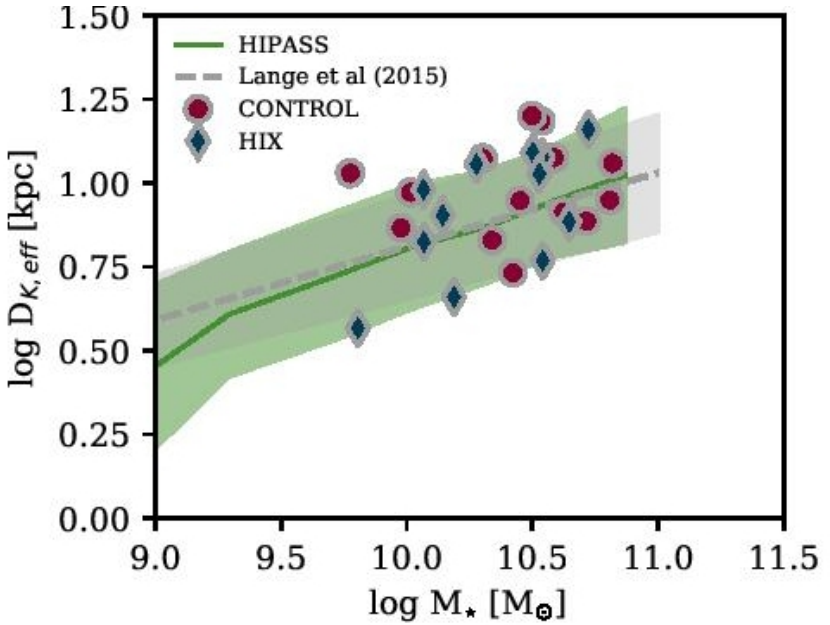

Figure 2. A stellar mass–size relation. The running average of the HIPASS parent sample is shown as the solid, green line, with the $\pm 1\,\sigma$ scatter as the green shaded area. For comparison the grey dashed line and grey shaded area give the mass–size relation and its errors for late-type galaxies from the GAMA survey (Lange et al. 2015). The control and HIX sample galaxies are shown as red circles and blue diamonds respectively. The HIX and control sample galaxies occupy a similar parameter space and follow the relation from the literature and the parent sample.

Свойства выборки: HI-диски НАМНОГО больше звездных

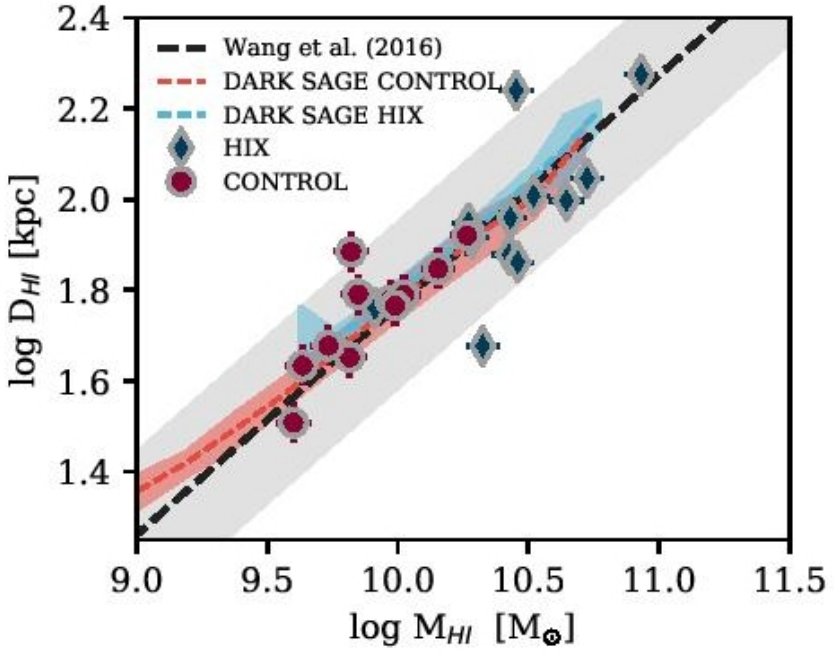

Figure 3. The relation between H I disc size and mass. Blue diamonds present the HIX sample and red circles the control sample. The grey dashed line is the relation found by Broeils & Rhee (1997), confirmed by Wang et al. (2016), where the grey shaded area covers their 3σ scatter of 0.18 dex. As in Fig. 1 light blue and orange dashed lines present DARK SAGE simulated galaxies and the shaded areas their respective 16 to 84 percentile ranges. H I masses and sizes of the HIX galaxies are consistent with the literature relation.

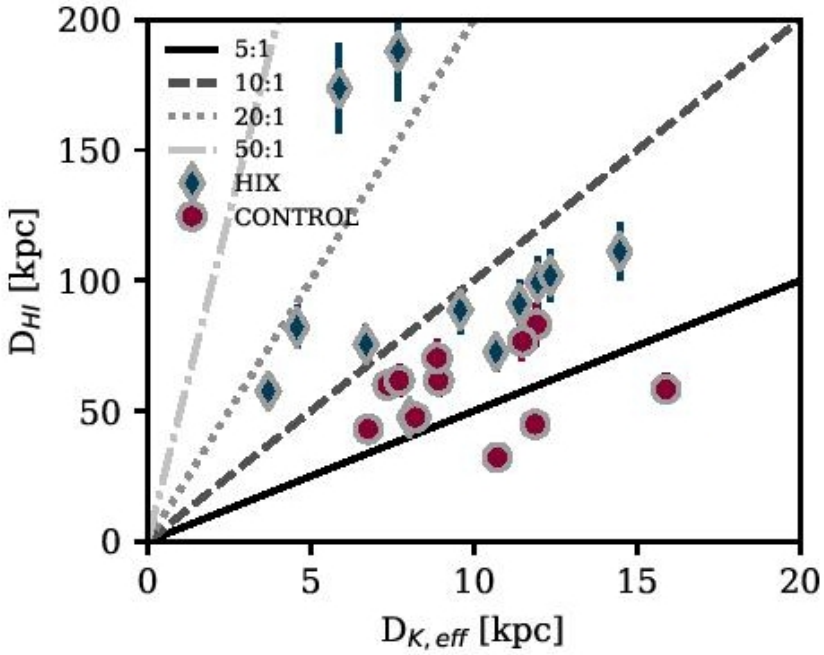

Figure 4. The relation between $R_{\rm HI}$ and the K-band effective radius. Blue diamonds present the HIX sample and red circles the control sample. Grey lines denote different ratios between the two sizes. At a given K-band effective radius, HIX galaxies tend to have larger H I disc sizes than the control sample.

Диски HI-rich галактик намного устойчивее контрольных

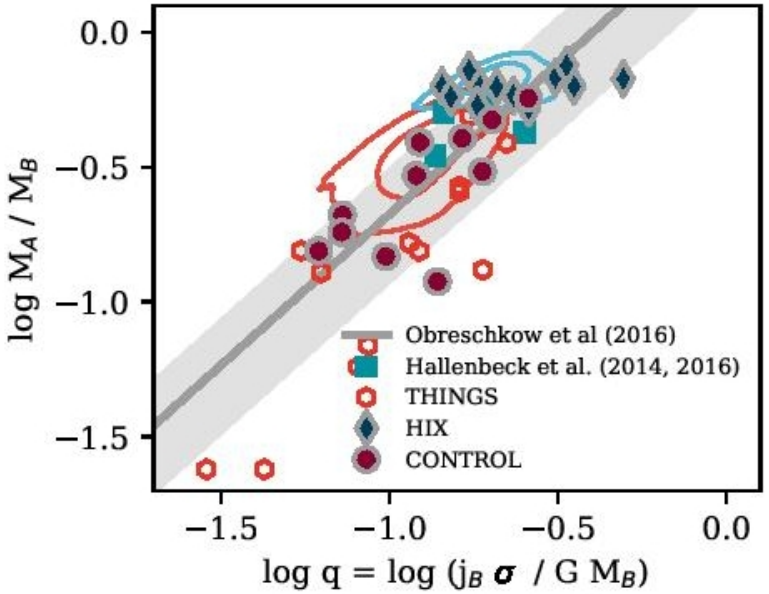

Figure 6. The atomic to baryonic gas ratio as a function of the global stability parameter. In addition to the data of the HIX (blue diamonds) and control sample (red circles), we also show data of THINGS galaxies (orange pentagons, Obreschkow & Glazebrook 2014) and HighMass galaxies (light blue squares). The orange and light blue contours encompass 68 and 95 per cent of the simulated control and HIX galaxies from DARK SAGE (for more details see Sec. 4). The data of observed and simulated galaxies agree with the analytical model of Obreschkow et al. (2016).

Потому и SF подавлено

Astro-ph: 1802.04798

AFTER THE FALL: THE DUST AND GAS IN E+A POST-STARBURST GALAXIES

A. Smercina[1,2], J.D.T. Smith[2,3], D.A. Dale[4], K.D. French[5,6,#], K.V. Croxall[7], S. Zhukovska[8], A. Togi[9], E.F. Bell[1], A.F. Crocker[10], B.T. Draine[11], T.H. Jarrett[12], C. Tremonti[13], Yujin Yang[14], A.I. Zabludoff[6]

[1]Department of Astronomy, University of Michigan, Ann Arbor, MI 48109, USA; asmerci@umich.edu

[2]Ritter Astrophysical Research Center, University of Toledo, Toledo, OH 43606, USA

[3]Max-Planck-Institut für Astronomie, Königstuhl 17, D-69117 Heidelberg, Germany

[4]Department of Physics & Astronomy, University of Wyoming, Laramie, WY 82071, USA

[5]Observatories of the Carnegie Institute for Science, 813 Santa Barbara Street, Pasadena, CA 91101, USA

[6]Department of Astronomy, University of Arizona, Steward Observatory, Tucson, AZ 85721, USA

[7]Illumination Works LLC, 5550 Blazer Parkway, Suite 150, Dublin, OH 43017

[8]Max-Planck Institut für Extraterrestrische Physik, Giessenbachstr. 1, 85748 Garching, Germany

[9]Department of Physics and Astronomy, University of Texas at San Antonio, One UTSA Circle, San Antonio, TX 78249, USA

[10]Department of Physics, Reed College, Portland, OR 97202, USA

[11]Department of Astrophysical Sciences, Princeton University, Princeton, NJ 08544, USA

[12]Department of Astronomy, University of Cape Town, Rondebosch 7701 South Africa

[13]Department of Astronomy, University of Wisconsin–Madison, Madison, WI 53706, USA

[14]Korea Astronomy and Space Science Institute, 776 Daedeokdae-ro, Yuseong-gu, Daejeon 34055, Korea

ABSTRACT

The traditional picture of post-starburst galaxies as dust- and gas-poor merger remnants, rapidly transitioning to quiescence, has been recently challenged. Unexpected detections of a significant ISM in

Выборка

2. SAMPLE SELECTION

The parent sample of this survey was drawn from the Sloan Digital Sky Survey (SDSS) Data Release 5 (DR5). Sources were required to possess Hα equivalent widths (EQWs) < 3 Å (vs. typically $\gg$10 Å in normal star-forming galaxies) and Lick Hδ absorption indices > 4 Å, defining a parent sample of 1122 galaxies. Sources were fitted using Bruzual & Charlot (2003) stellar population synthesis models, to infer burst properties and post-burst ages. The majority of sources have existing GALEX NUV and FUV wavelengths coverage, the addition of which significantly alleviates age-reddening degeneracies. French et al. (2017, submitted) details the UV-optical spectrophotometric fitting methodology which provides, among other physical parameters, reliable post-starburst ages over the range 100-1500 Myr, with typical uncertainties of ~20%.

Осталось 33 галактики

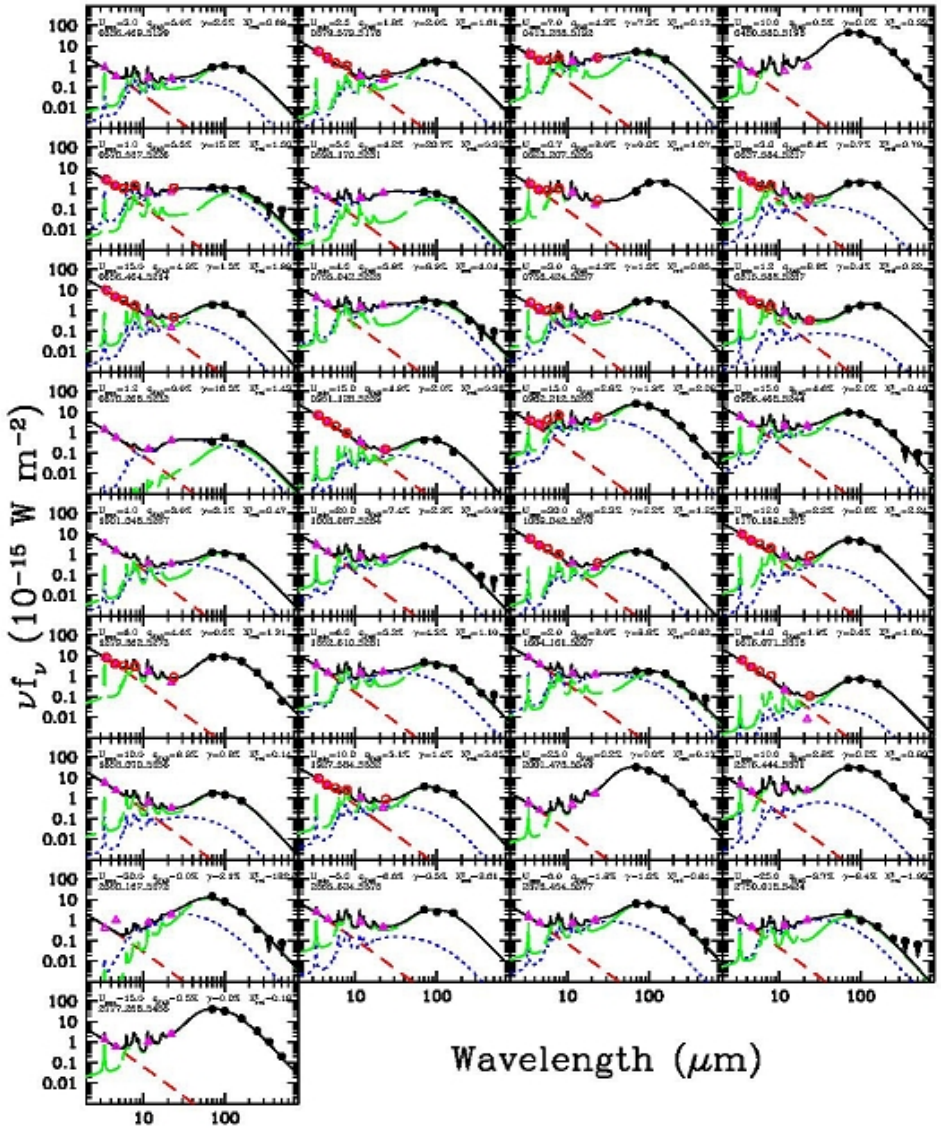

Три компонента спектра: звездный, пылевой и диффузная среда

Температура пыли повышена

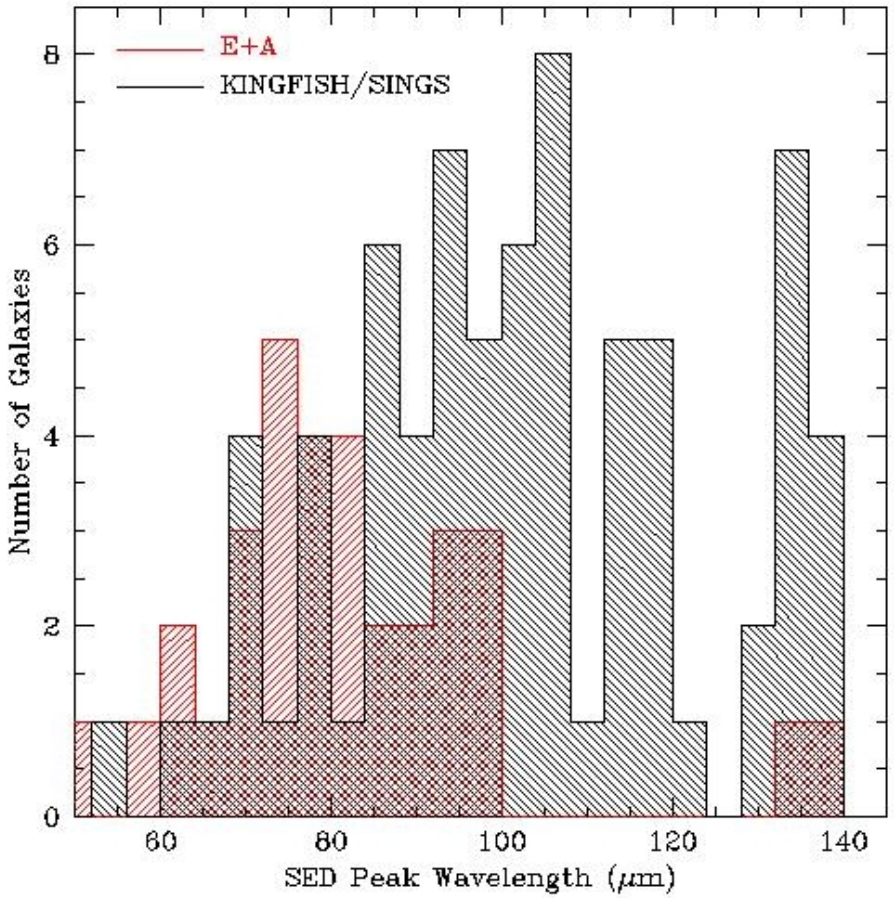

Figure 3. Comparison histograms of the SED peak wavelength for the E+A and matched KINGFISH/SINGS samples. Note that the 13 SINGS/KINGFISH sources with peaks ∼130 µm are low-metallicity dwarf galaxies. The E+A sample has infrared SED's that peak at ∼70 µm, much warmer than the KINGFISH/SINGS mean of ∼100 µm.

Есть линии PAH и теплого H_2 , но нет небулярных линий (или слабы)

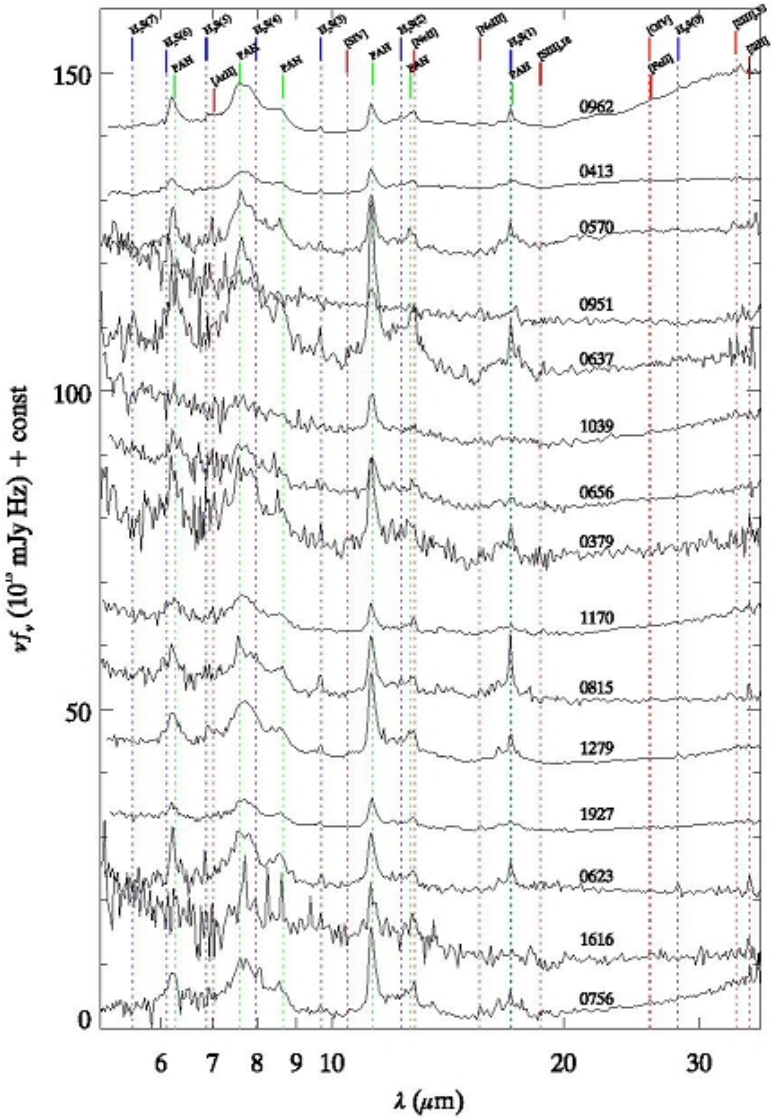

Дефицит линий [CII] и [OI]

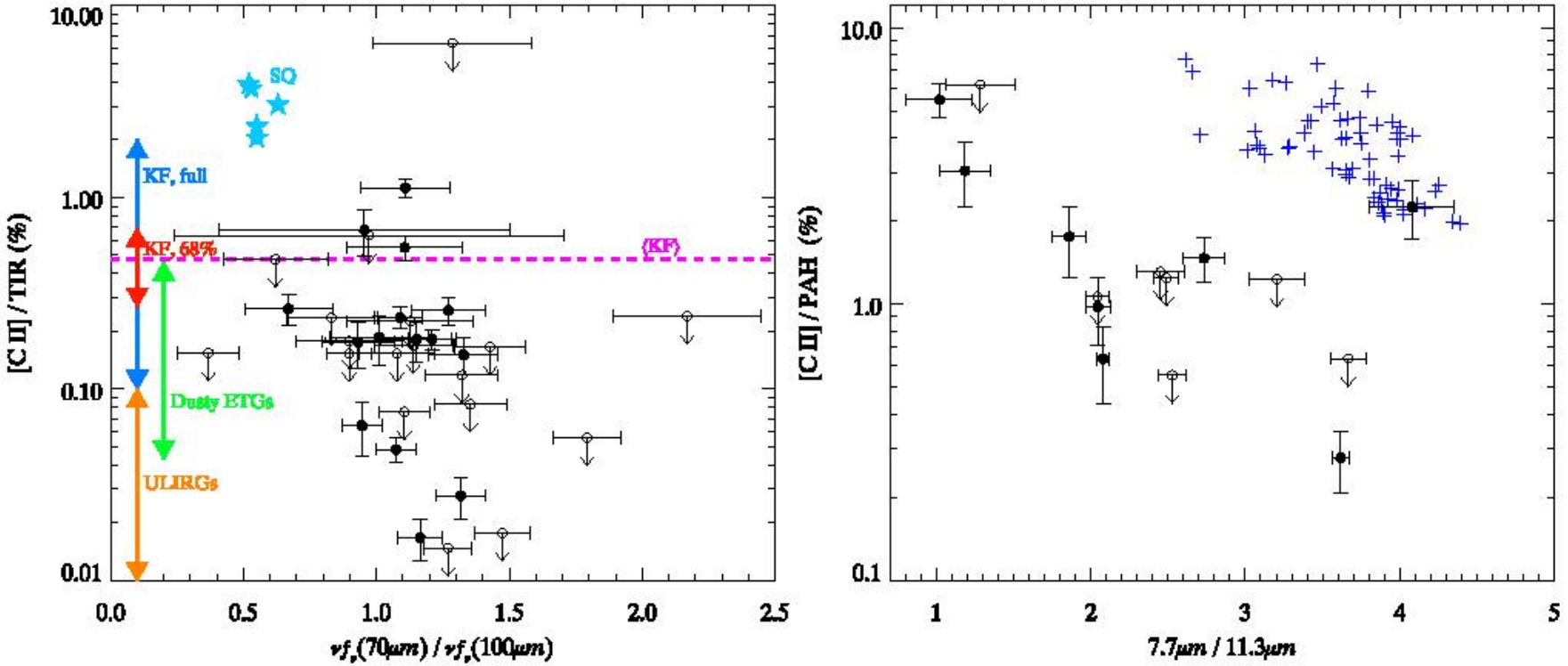

Figure 13. Left: The [C II] deficit ([C II]/ TIR) plotted as a function of 70 µm/100 µm color. The E+As are shown as black, filled circles, where open circles with downward arrows denote 3σ upper limits. The double-headed arrows denote the ranges of various comparison samples: the KINGFISH (Smith et al. 2017) full range (blue), 68% range (red), and mean (magenta), dusty ETGs (green), and GOALS ULIRGs (orange; Díaz-Santos et al. 2013, assuming a multiplicative factor of 2 for FIR-to-TIR conversion). We also show individual regions of the inter-galaxy shock ridge in Stephan's Quintet (light blue stars; Appleton et al. 2013). Right: [C II]-to-total PAH emission as a function of the 7.7 µm/11.3 µm PAH band ratio. The E+As follow the same schema as the left figure. The blue plus symbols correspond to resolved regions within the star-forming galaxies NGC 1097 and NGC 4559 (Croxall et al. 2012). The E+As seem to posses significantly deeper [C II] deficits than most normal, star-forming

Если определять SFR по линиям неона, то сильно выпадают вниз от главной последовательности

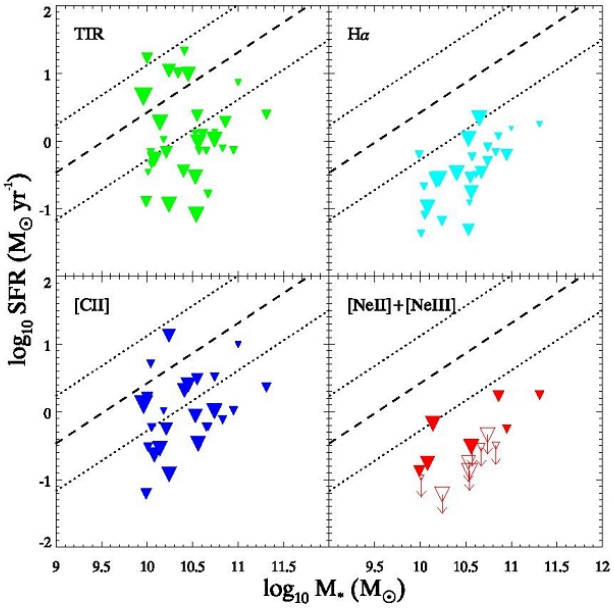

Figure 18. SFR rate vs. stellar mass. For the E+A sample, we plot each of our derived SFRs in a separate panel: TI (upper left; green), [C II] (bottom left; blue), and Neon (bottom right; red). We also include Hα (FYZ15, upper right; cyan Symbol size is scaled linearly with post-burst age (oldest have largest symbols). SFR limits are denoted by downward arrow The dashed and dotted lines show the WISE best-fit and full range, respectively, to late-type galaxies in the GAMA G12 fiel (Jarrett et al. 2017) — the star-forming main sequence. Hα SFRs have been excluded for the seven sources with high inferre extinction. Though there is considerable scatter among different tracers, the E+As overwhelmingly lie below the star-formin

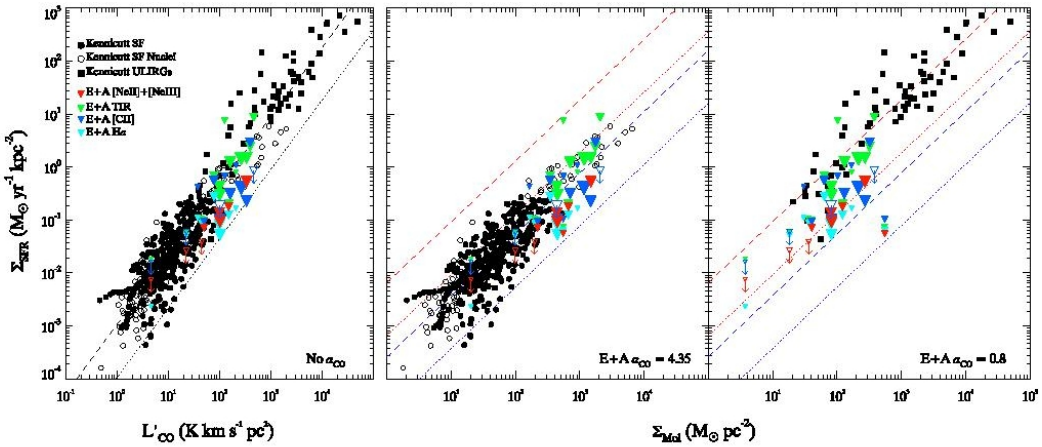

Figure 19. The Kennicutt Schmidt star-formation diagram. SFR surface density is plotted as a function of CO surface brightness (left) and molecular gas surface density (center, right). Galaxies with CO limits have been excluded, as have $\Sigma_{\rm SFR}(\rm H\alpha)$ for the seven sources with significant inferred extinction. The one exception is 0815, which, though it is not detected in CO(1–0), does have a reliable molecular mass from fitting of its H_2 temperature distribution (§ 4.6). The comparison sample is derived from the original sample of Kennicutt (1998), composed of star-forming galaxies (black, filled circles) with $\alpha_{co} = 4.35$, star-forming galaxy nuclei (black, open circles) with $1 \leq \alpha_{\rm CO} \leq 3.6$, and ULIRGs (black, filled squares) with $\alpha_{\rm CO} = 0.8$. The E+As are plotted assuming $\alpha_{\rm CO}$ factors of: (Left) None, (Center): 4.35, (Right): 0.8. Power-law fits to the comparison samples are shown in each panel as dashed lines: SF galaxies (blue) and ULIRGs (red). Lines with 10× lower normalization than each fit (but identical slopes) are shown as dotted lines, again with blue corresponding to SF galaxies and red to ULIRGs. Assuming $\alpha_{co} = 4.35$, the E+As are offset from SF galaxies by a factor of 5 when considering Neon SFRs. Assuming $\alpha_{co} = 0.8$, the E+As are offset from ULIRGs by a factor of 10 when considering Neon.